Polarization and Charge-Transfer Effects in Lewis Acid−Base Complexes

Yirong Mo and Jiali Gao*

Department of Chemistry and Minnesota Supercomputing Institute, University of Minnesota, Minneapolis, Minnesota 55455

Received: January 26, 2001; In Final Form: March 30, 2001

An interaction energy decomposition method has been used to investigate bonding interactions in a series of Lewis acid−base complexes. It was found that the bonding interaction of these donor−acceptor complexes can be divided into two main groups. The first involves weakly interacting complexes, which have characteristic interaction energies of 3−9 kcal/mol and monomer separations of 2.5−3.1 Å. The second group consists of strongly bonding complexes, which have bonding energies of greater than 20 kcal/mol with short interaction distances (1.6−2.0 Å) between the donor and acceptor molecule. The bonding interactions of group I complexes are primarily electrostatic in nature, whereas charge polarization and charge transfer between the two interacting monomers dominate the interaction in group II complexes. A good linear relationship is observed between the charge-transfer energy and the amount of charge-transfer from the donor to the acceptor species. Interestingly, the total bonding energy also correlates linearly with the polarization energy and charge-transfer energy. Thus, a correlation between the total binding energy and charge transfer may also be observed.

Introduction

Lewis acid and base complexes are characterized by interactions that lie between the bonding and nonbonding regimes and, thus, are of considerable interest in the understanding of the chemical bond.[1−4] This is illustrated by the remarkable observations that the bond length of the $(CH_3)_3N-BF_3$ adduct is 1.58 Å in the gas phase,[5] close to a fully formed chemical bond between boron and nitrogen,[6] whereas N_2-BF_3 has an observed bond distance of 2.88 Å,[7] corresponding to interactions of a van der Waals complex. Furthermore, medium effects are also critical in determining the bonding character of Lewis acid−base complexes due to enhanced charge transfer and polarization. For example, in solid state, X-ray and neutron diffraction experiments reveal an N−S distance of 1.771 Å for sulfamic acid H_3N-SO_3;[8,9] however, the bond length is increased to a value of 1.957 Å from the microwave spectroscopic experiment. The latter is also consistent with computational studies, giving a predicted value of 1.912−1.972 Å at the HF/6-31+G(2d) and CISD/6-31G(d) level of theory.[10−12]

These intriguing systems have been a subject of continuing experimental and theoretical studies.[13] The key question in these investigations is the nature of the interaction between a donor and an acceptor molecule, and the correlation between charge transfer with bonding characters such as interaction energy and bond length.[14] This interest stems from the original proposal by Mulliken,[15] who related the formation of donor−acceptor complex to the degree of charge transfer from the highest occupied molecular orbital (HOMO) of the donor to the lowest unoccupied molecular orbital (LUMO) of the acceptor. Although a linear correlation between bonding energy and the amount of charge transferred has been observed for certain complexes,[16] this relationship does not exist in other systems.[17,18]

The primary goal of this study is to investigate the effects of charge transfer and charge polarization on the formation and stability of Lewis acid and base complexes.[19] We employ an energy decomposition method, recently developed in our laboratory, to determine specific energy terms.[20] Findings from this analysis provide insights into the interplay of electron transfer, charge polarization and electrostatic interactions in determining the bonding character of a donor−acceptor complex.[21] Recently, this energy decomposition method has been applied to interpret molecular dipole moments in a series of nitrogen−boron and nitrogen−sulfur complexes,[22] which have been experimentally studied by the Leopold group.[10,23−26] The energy decomposition results revealed specific contributions to the dipole moment of the donor−acceptor adducts from polarization and charge-transfer effects. In this paper, we extend the analysis to provide insight on the nature of the bonding interaction in these complexes.

In the following, we first briefly summarize the energy decomposition method used in the present analysis. This is followed by results and discussion. The paper concludes with a summary of major findings of this work.

Theoretical Background

(1) Energy Decomposition. The total interaction energy (ΔE_{int}) for a bimolecular complex, DA, is defined as the difference between the energy of the complex and the sum of the energies of the two separated monomers, D and A. Computationally, ΔE_{int} can be separated into a Hartree−Fock (HF) interaction energy term, ΔE_{HF}, and a correction component due to electron correlation and dispersion effects. The latter is approximated by the Moller−Plesset second-order perturbation theory (MP2), $\Delta\Delta E_{MP2}$. Thus,

$$\Delta E_{int} = \Delta E_{HF} + \Delta\Delta E_{MP2} \quad (1)$$

The Hartree−Fock interaction energy is determined as follows:

$$\Delta E_{HF} = E_{HF}[\Psi(DA)] - E^{\circ}_{HF}[\Psi^{\circ}(D^{\circ})] - E^{\circ}_{HF}[\Psi^{\circ}(A^{\circ})] + \Delta E_{BSSE} \quad (2)$$

where ΔE_{BSSE} is the Boys−Bernardi counterpoise (CP) correction for the basis set superposition error (BSSE),[27] $E[\Psi(DA)]$

10.1021/jp010348w CCC: $20.00
Published on Web 06/01/2001

is the Hartree−Fock energy of the complex DA, and $E[\Psi°(D°)]$ and $E[\Psi°(A°)]$ are, respectively, energies for monomers D° and A° at their equilibrium geometries.

Electron correlation and dispersion interactions are approximated by MP2, and $\Delta\Delta E_{MP2}$ is the difference between the MP2 and HF interaction energy:

$$\Delta\Delta E_{MP2} = [E_{MP2}(DA) - E_{MP2}(D°) - E_{MP2}(A°)] - \Delta E_{HF} + \Delta E_{BSSE} \quad (3)$$

In eq 3, $E_{MP2}(DA)$, $E_{MP2}(D°)$, and $E_{MP2}(A°)$ are MP2 energies for the complex and individual monomers. Equation 3 also implies that the BSSE correction is the same at the MP2 level as that at the HF level.[28] However, it should be emphasized that this assumption is not always fulfilled, particularly when small basis sets are used. The present treatment should not affect the discussion on the trend of energy decomposition analysis.

In the present energy decomposition method we employ a block-localized wave function (BLW) technique[29,30] that has been described previously. Then, a series of intermediate wave functions are constructed to represent various charge states. Thus, the HF interaction energy is partitioned into a sum of geometry distortion (ΔE_{dist}), electrostatic (ΔE_{es}), exchange repulsion (ΔE_{ex}), polarization (ΔE_{pol}), and charge transfer (ΔE_{ct}) terms:

$$\Delta E_{HF} = \Delta E_{dist} + \Delta E_{es} + \Delta E_{ex} + \Delta E_{pol} + \Delta E_{ct} \quad (4)$$

The BLW energy decomposition method is analogous to the traditional Morokuma analysis[31] in definition of the energy terms but differs in the computational procedure. In comparison with the Morokuma decomposition scheme, the BLW decomposition method exhibits much less dependency on the basis set used in the calculation.[20]

Specifically, the ΔE_{dist} term in eq 4 is the distortion energy of the monomers, corresponding to the change from the equilibrium geometry of isolated monomers D° and A° to that in the configuration (D and A). Therefore,

$$\Delta E_{dist} = E_{HF}[\Psi°(D)] + E_{HF}[\Psi°(A)] - E_{HF}[\Psi°(D°)] - E_{HF}[\Psi°(A°)] \quad (5)$$

where the superscript specifies that the wave function is determined for an isolated monomer, D° and A° indicate equilibrium monomer geometries, and D and A denote the monomer geometry in the complex conformation.

The electrostatic term is the Coulombic interaction energy between the two monomers possessing the gas-phase (or unperturbed) charge distribution, and it is determined by the energy difference between a reference electronic state without quantum mechanical exchange and the energies of the monomers.

$$\Delta E_{es} = E(\Phi°_H[D,A]) - E_{HF}[\Psi°(D)] - E_{HF}[\Psi°(A)] \quad (6)$$

where the wave function for this reference state corresponds to a Hartree product of the two monomer Slater determinants:

$$\Phi°_H[D,A] = \Psi°(D)\Psi°(A) \quad (7)$$

To evaluate the exchange energy due to the Pauli exclusion principle, we define the intermediate wave function, $\Phi°_{DA}$, which is the antisymmetrized form of the Hartree product of eq 7. Thus,

$$\Phi°_{DA} = \hat{A}\{\Phi°_H[D,A]\} = \hat{A}\{\Psi°(D)\Psi°(A)\} \quad (8)$$

and

$$\Delta E_{ex} = E(\Phi°_{DA}) - E(\Phi°_H[D,A]) \quad (9)$$

It is important to notice in eq 8 that molecular orbitals on the two individual monomers are nonorthogonal, and the evaluation of the exchange energy by eq 9 must take this fact into account.

The polarization energy is determined by optimizing the nonorthogonal wave function of eq 8 using the BLW method.

$$\Delta E_{pol} = E(\Phi_{DA}) - E(\Phi°_{DA}) \quad (10)$$

where the wave function Φ_{DA} is defined as follows:

$$\Phi_{DA} = \hat{A}\{\Psi(D)\Psi(A)\} \quad (11)$$

It should be noted that in the BLW optimization step, the expansion of molecular orbitals of each monomer are restricted to be over basis functions that are located on atoms of that monomer. The orbital optimization is carried out in the presence of the field of the other monomer with nonorthogonal orbital overlap. Therefore, the degree sign is removed from the polarized monomer wave functions.

Finally, removing the restriction of molecular orbital expansion space in eq 11 leads to the optimized HF wave function of the DA dimer. The energy change accompanying this process is defined as the charge-transfer energy because only in this step does charge delocalization occur in the computation:

$$\Delta E_{ct} = E_{HF}[\Psi(DA)] - E[\Phi_{DA}] + \Delta EB_{BSSE} \quad (12)$$

Note that the BSSE correction is also included in the charge-transfer term since it includes expansion of the orbital space similar to the change on going from Φ_{DA} to $\Psi(DA)$.

The polarization and charge-transfer terms defined in eqs 10 and 12 are intimately related because both interactions result from charge reorganization within the molecular complex. The polarization energy as defined in eq 10 describes the energy change due to intramolecular charge delocalization, whereas the charge-transfer term of eq 12 accounts for intermolecular charge migration. By definition, both ΔE_{pol} and ΔE_{ct} terms provide stabilization of the molecular system and are thus always negative. In the original Morokuma analysis,[31] charge-transfer and polarization energies are determined by formulating an interaction Fock matrix that includes interactions between occupied and virtual orbitals of individual monomers. Consequently, there is significant overlap between the two components, sometimes resulting in a large, unphysical coupling term, ΔE_{cp}, as the size of the basis function increases. In our BLW-energy decomposition scheme, specific intermediate wave functions are defined, avoiding the problem of a coupling energy term that occurs in the Morokuma analysis. Furthermore, the availability of intermediate wave functions allows us to estimate intermediate molecular dipole moments and charge population, which are of interest in the understanding of bonding interactions.

(2) Computational Details. All calculations are carried out using the BLW program[32] and the GAUSSIAN package.[33] Monomer and bimolecular complex geometries are optimized at the HF/6-31G(d) and HF/6-311+G(d,p) level, while the same basis set is used in MP2 and energy decomposition calculations. The Boys−Bernardi counterpoise method[27] is used to correct for basis set superposition error, which is included as part of the charge-transfer energy in the BLW-energy decomposition

TABLE 1: Computed Total Interaction Energies and Energy Components from the Block-Localized Wave Function Decomposition Analysis Using the HF/6-31G(d) Basis Function (kcal/mol)

species	ΔE_{dist}	ΔE_{es}	ΔE_{ex}	ΔE_{es+ex}	ΔE_{pol}	ΔE_{ct}	ΔE_{MP2}	ΔE_{int}
$N_2\cdots SO_3$	0.0	−2.2	1.9	−0.3	−0.5	−0.4	−1.6	−2.7
$HCN\cdots SO_3$	0.4	−10.9	8.4	−2.5	−1.8	−1.8	−1.3	−7.1
$MeCN\cdots SO_3$	0.7	−14.4	11.7	−2.7	−2.5	−2.6	−1.4	−8.7
$H_3N\cdots SO_3$	9.2	−113	156	42.9	−23.9	−47.2	−0.8	−19.8
$Me_3N\cdots SO_3$	17.3	−128	191	63.0	−43.8	−62.8	−6.3	−32.6
$HCN\cdots BF_3$	0.7	−7.6	5.1	−2.5	−0.9	−0.6	−1.5	−4.9
$MeCN\cdots BF_3$	1.2	−10.4	7.2	−3.2	−1.4	−1.0	−1.6	−5.9
$H_3N\cdots BF_3$	24.4	−103	112	9.8	−20.5	−29.6	−5.3	−21.2
$Me_3N\cdots BF_3$	31.8	−103	119	15.8	−32.8	−32.6	−10.8	−28.6
$H_3N\cdots BH_3$	13.6	−88.7	99.4	10.7	−18.9	−26.5	−10.7	−31.7
$Me_3N\cdots BH_3$	16.9	−91.4	107.3	15.9	−27.1	−28.9	−15.7	−39.6
$H_3N\cdots BMe_3$	15.5	−82.5	102	19.1	−18.0	−23.2	−13.0	−19.5
$Me_3N\cdots BMe_3$	22.7	−67.7	84.9	17.2	−18.6	−21.3	−21.3	−21.4

TABLE 2: Computed Total Interaction Energies and Energy Components from the Block-Localized Wave Function Decomposition Analysis Using the HF/6-311+G(d,p) Basis Function (kcal/mol)

species	ΔE_{dist}	ΔE_{es+ex}	ΔE_{pol}	ΔE_{ct}	ΔE_{MP2}	ΔE_{int}
$N_2\cdots SO_3$	0.0	−0.4	−0.5	−0.1	−1.4	−2.4
$HCN\cdots SO_3$	0.4	−2.0	−2.3	−1.9	−1.0	−6.8
$MeCN\cdots SO_3$	0.8	−1.4	−3.6	−3.1	−1.2	−8.5
$H_3N\cdots SO_3$	9.9	54.6	−29.3	−53.3	−1.6	−19.7
$Me_3N\cdots SO_3$	17.8	69.1	−49.2	−65.0	−5.9	−33.2
$HCN\cdots BF_3$	0.6	−2.5	−1.1	−0.6	−1.0	−4.6
$MeCN\cdots BF_3$	1.3	−2.9	−1.8	−1.2	−1.2	−5.8
$H_3N\cdots BF_3$	26.9	21.1	−29.0	−36.1	−4.7	−21.8
$Me_3N\cdots BF_3$	34.7	20.6	−38.8	−37.3	−9.6	−30.4
$H_3N\cdots BH_3$	14.0	23.9	−26.9	−30.5	−11.1	−30.6
$Me_3N\cdots BH_3$	17.2	23.1	−33.0	−30.6	−17.2	−40.5
$H_3N\cdots BMe_3$	15.4	28.9	−23.2	−26.3	−13.5	−18.7
$Me_3N\cdots BMe_3$	22.3	21.3	−21.4	−22.2	−23.5	−23.5

analysis. Since we are able to obtain the intermediate wave function Φ_{DA} (eq 11), which has charge-transfer effects "turned off", comparison of results from population analyses over this wave function and the fully delocalized adiabatic wave function Ψ(DA) provide insight on the charge-transfer mechanism. Moreover, the amount of charges transferred between D and A, which is the difference between the populations of D in Φ_{DA} and Ψ(DA), is expected to correlate with the corresponding charge-transfer stabilization energy following the ideas of Mulliken. For this purpose, both Mulliken population and Weinhold's natural population analysis (NPA) are employed.[34] The latter approach is known for its stability with the size of basis function used in comparison with the Mulliken population analysis.

Results and Discussion

Total interaction energies and energy components computed using the 6-31G(d) and 6-311+G(d,p) basis sets from the BLW decomposition analysis are summarized in Tables 1 and 2 for a series of Lewis acid−base complexes. The total interaction energies determined from these two different basis sets are in remarkable agreement with a root-mean-square difference of only 0.9 kcal/mol. Roughly, these bimolecular complexes may be grouped into two categories according to the nature and strength of binding interactions. Complexes involving weak Lewis bases such as N_2, HCN, and CH_3CN typically show binding energies in the range 3−9 kcal/mol, whereas strong Lewis bases, including ammonia and trimethylamine, form complexes with binding energies greater than 20 kcal/mol. A rough correlation exists between interaction energy and the optimized intermolecular distances between the electron donor and acceptor atoms (Table 3). For weak complexes, intermolecular distances are 2.51−3.06 Å, whereas 1.68−1.95 Å are found for strongly interacting dimers. This is further reflected in the computed monomer distortion energies due to greater geometrical variations at shorter interacting distances in the complex. In the weakly interacting complexes, the distortion energies are only 0−1 kcal/mol. On the other hand, they are 9−35 kcal/mol for strongly bonded complexes, which are also reflected by the change in bond angle in Table 3.

TABLE 3: Computed Intermolecular Distances (Ångstroms) and Bond Angles (Degrees) at the HF/6-31G(d) Level

complex	R_{XY}	θ (donor)	θ (acceptor)
$N_2\cdots SO_3$	3.058	180.0	90.3
$HCN\cdots SO_3$	2.704	180.0	91.5
$MeCN\cdots SO_3$	2.620	180.0	92.0
$H_3N\cdots SO_3$	1.951	109.7	97.5
$Me_3N\cdots SO_3$	1.898	108.7	99.4
$HCN\cdots BF_3$	2.601	180.0	92.4
$MeCN\cdots BF_3$	2.506	180.0	93.4
$H_3N\cdots BF_3$	1.693	110.6	103.6
$Me_3N\cdots BF_3$	1.679	109.1	105.0
$H_3N\cdots BH_3$	1.689	110.9	104.3
$Me_3N\cdots BH_3$	1.677	109.3	105.2
$H_3N\cdots BMe_3$	1.739	111.1	103.9
$Me_3N\cdots BMe_3$	1.825	110.5	106.5

Dispersion and electron correlation effects, estimated at the MP2/6-31G(dp)//HF/6-31G(d) level, are significant for complexes that contain trimethyl groups, ranging from −10.8 to −21.3 kcal/mol. In fact, for the two complexes, $H_3N-B(CH_3)_3$ and $(CH_3)_3N-B(CH_3)_3$, the binding energies are nearly entirely due to electron correlation and dispersion interactions. An exception is the complex between ammonia and boron hydride, which does not have a methyl group but has an electron correlation correction of −10.7 kcal/mol. In this case, we have also carried out MP2, MP4, and CCSD(T) calculations using the 6-311+G(d,p) basis function, and binding energies of −11.1, −10.8, and −10.6 kcal/mol are obtained, respectively. The MP2 calculation yields a slight overestimate of the binding energy compared to higher levels of theory. MP2 and MP4 energies computed using the 6-31G(d) basis set for all complexes are within 0.7 kcal/mol.

In all cases, there is a compensating effect between electrostatic and exchange energies. The electrostatic term is attractive and becomes more negative as the monomer separation distance decreases because of an increased penetration of the electron cloud of each monomer into regions of the nuclei of the other monomer. The same charge penetration effect also leads to enhanced overlap of occupied orbitals, giving rise to greater exchange repulsion interactions. The sum of these two terms corresponds to the net interaction energy due to the permanent (gas phase) charge distribution of the two free monomers in

TABLE 4: Comparison of Energy Decomposition Results Obtained from the Present Block-Localized Wavefunction Method and from the Morokuma Analysis (Energies in kcal/mol)

	6-31G(d)						6-311+G(d,p)					
	Morokuma analysis			BLW decomposition			Morokuma analysis			BLW decomposition		
complex	ΔE_{pol}	ΔE_{ct}	ΔE_{cp}[a]	ΔE_{pol}	ΔE_{ct}	ΔE_{BSBE}	ΔE_{pol}	ΔE_{ct}	ΔE_{cp}[a]	ΔE_{pol}	ΔE_{ct}	ΔE_{BSBE}
$N_2\cdots SO_3$	−0.5	−1.2	0.2	−0.5	−0.4	0.6	−2.1	−0.8	1.5	−0.5	−0.1	0.7
$HCN\cdots SO_3$	−2.1	−3.5	0.7	−1.8	−1.8	1.3	−11.8	−3.9	10.3	−2.3	−1.9	1.1
$MeCN\cdots SO_3$	−3.1	−4.7	1.1	−2.5	−2.6	1.6	−81	−180	253	−3.6	−3.1	1.4
$H_3N\cdots SO_3$	−43.1	59.9	27.0	−23.9	−47.2	4.9	−271	−391	576	−29.3	−53.3	3.4
$Me_3N\cdots SO_3$	−97.5	−83.9	68.2	−43.8	−62.8	6.5	−1082	−113	1076	−49.2	−65.0	4.8
$HCN\cdots BF_3$	−1.1	−1.9	0.2	−0.9	−0.6	1.2	−3.0	−1.3	2.2	−1.1	−0.6	0.6
$MeCN\cdots BF_3$	−1.7	−0.25	0.4	−1.4	−1.0	1.4	−9.7	−2.5	8.4	−1.8	−1.2	0.7
$H_3N\cdots BF_3$	−38.0	−39.7	23.0	−20.5	−29.6	4.6	*b*	*b*	*b*	−29.0	−36.1	1.9
$Me_3N\cdots BF_3$	−69.0	−48.6	45.7	−32.8	−32.6	6.5	−691	−579	1190	−38.8	−37.3	2.8
$H_3N\cdots BH_3$	−27.7	−32.4	12.2	−18.9	−26.5	2.5	−49.2	−61.1	51.8	−26.9	−30.5	1.1
$Me_3N\cdots BH_3$	−50.7	−38.0	30.4	−27.1	−28.9	2.4	−417	−434	786	−33.0	−30.6	1.0
$H_3N\cdots BMe_3$	−33.6	−36.7	25.6	−18.0	−23.2	3.4	*b*	*b*	*b*	−23.2	−26.3	1.2
$Me_3N\cdots BMe_3$	−30.7	−30.1	18.2	−18.6	−21.3	2.8	*b*	*b*	*b*	−21.4	−22.2	1.2

[a] Polarization-charge-transfer coupling energy. [b] Morokuma analysis did not converge using GAMESS.

the complex configuration. Interestingly, for weakly interacting complexes, this zeroth order, or vertical electrostatic interaction is attractive and makes major contributions to the total binding energy. However, at short intermolecular distances, the exchange repulsion is more significant and the net vertical (or electrostatic) interaction energy is in fact repulsive (the ΔE_{es+ex} term in Tables 1 and 2). Concomitantly, polarization and charge-transfer energies are greatly increased, which become the predominant contributing components in the total binding energy.

The interaction energy decomposition analyses indicate that there are two different binding modes in Lewis acid−base complexes, resulting in weakly and strongly interacting pairs, as noted above. Long-range electrostatic attraction is the dominant force for the weakly bonded complex with relatively small polarization and charge-transfer contribution. Alternatively, there is significant HOMO−LUMO mixing at short intermolecular separations, resulting in large polarization and charge-transfer energies, which are the driving force for forming strong Lewis acid−base complexes (Tables 1 and 2). The greater extent of orbital overlap also leads to significant electrostatic and exchange repulsion components. In this class, the electrostatic and exchange energies are 2 orders of magnitude greater than the corresponding terms in weak complexes, although the net combined electrostatic and exchange effects are clearly repulsive in these strongly bonded complexes.

The results obtained from our BLW decomposition scheme and from the Morokuma analysis depend on the basis set employed in the calculation, although our method shows a lesser tendency of divergence. This trend is shown in Table 4, which compares the polarization and charge-transfer terms determined using the two methods at the 6-31G(d) and 6-311+G(d,p) level. The electrostatic and exchange terms from the BLW and Morokuma analysis are identical (Tables 1 and 2). In making this comparison, one should keep in mind that the correction for basis set superposition error has been included in the charge-transfer term in the BLW method, whereas it is ignored in the Morokuma analysis. Furthermore, there is a coupling term between polarization and charge transfer in the latter analysis. The BLW method does not contain such a coupling term because explicit intermediate wave functions have been defined in the calculation. Using the smaller 6-31G(d) basis set, the Morokuma analysis yields results in good accord with the BLW approach for weak donor−acceptor complexes. For strong interactions, there is always a large coupling term in the Morokuma analysis, and such a term becomes unphysical even for weak interactions using a larger basis set. On the other hand, the computed polarization and charge-transfer terms, although also basis-set dependent, are relatively stable from the BLW decomposition analysis. The BSSE correction makes a modest contribution to the charge-transfer energy, but it does not alter the qualitative trends and the correction is reduced when a larger basis function is used (Table 4).

Computed dipole moments are listed in Table 5. Since molecular wave functions are explicitly defined in the present BLW energy decomposition analysis, it allows us to determine the individual monomer as well as the complex dipole moments at different charge states. Specifically, we have computed the free monomer dipole moments at the equilibrium geometry, $\mu°(X°)$, and at the distorted complex geometry, $\mu°(X)$, both using the gas-phase HF wave function. The monomer dipole moment in the presence of the other monomer in the complex, $\mu_{BLW}(X)$, is obtained by using the individual component $\Psi(X)$ of the BLW wave function Φ_{DA} defined in eq 11. The difference is the induced dipole moment for the monomer due to polarization.

$$\Delta\mu_{pol}(X) = \mu_{BLW}(X) - \mu°(X) \tag{13}$$

Here, X represents either a Lewis acid (A) or a base (D) in a complex. In addition, the intermediate molecular dipole moment for the entire DA complex, $\mu_{BLW}(DA)$, can be determined using the wave function Φ_{DA} (eq 11). Here, we note that $\mu_{BLW}(DA) \approx \mu_{BLW}(D) + \mu_{BLW}(A)$ because there is no charge-transfer component in Φ_{DA}. The charge-transfer contribution to the total molecular dipole moment of the DA complex is

$$\Delta\mu_{CT}(DA) = \mu_{HF}(DA) - \mu_{BLW}(DA) \tag{14}$$

where $\mu_{HF}(DA)$ is the HF dipole moment for the complex DA from the wave function $\Psi(DA)$.

Table 6 listed the contributions from the polarization and the charge-transfer effects to the dipole moment of the adduct. Overall, the polarization of the monomers (especially the Lewis acids) and the charge-transfer effects make nearly equal contributions to the total induced dipole moment in a Lewis acid−base complex over the sum of dipole moments of separated monomers. As a result, the experimental estimation of the charge-transfer effect based on the nuclear hyperfine parameters,[35−37] which omit the polarization effect, will remarkably overestimate the degree of charge transfer.

To gain additional insight into the polarization and charge-transfer effects in the complex, we take BH_3NH_3 as an example

TABLE 5: Computed Dipole Moments for Separated Monomers at the Equilibrium Geometry, $\mu°$(A°), and at the Distorted Complex Geometry, $\mu°$(A); Polarized Monomer Dipoles, μ_{BLW}(A), and Total Complex Dipoles, μ_{BLW}(AB), without Charge Transfer; and Total Complex Dipole Moments, μ_{HF}(AB), That Include Both Polarization and Intermolecular Charge Transfer (Dipole Moments in Debye)

	Lewis base B			Lewis acid A[a]			
species	$\mu°$(B°)	$\mu°$(B)	μ_{BLW}(B)	$\mu°$(A)	μ_{BLW}(A)	μ_{BLW}(AB)	μ_{HF}(AB)
$N_2\cdots SO_3$	0.0	0.0	0.28	0.0	0.11	0.41	0.46
$HCN\cdots SO_3$	3.21	3.21	3.79	0.22	0.55	4.35	4.57
$MeCN\cdots SO_3$	4.04	4.03	4.83	0.30	0.71	5.55	5.87
$H_3N\cdots SO_3$	1.92	1.79	2.68	1.09	2.14	4.80	6.88
$Me_3N\cdots SO_3$	0.74	0.94	2.83	1.35	2.67	5.49	7.86
$HCN\cdots BF_3$	3.21	3.21	3.61	0.31	0.50	4.11	4.22
$MeCN\cdots BF_3$	4.04	4.04	4.61	0.42	0.66	5.27	5.42
$H_3N\cdots BF_3$	1.92	1.85	2.75	1.85	2.52	5.17	6.17
$Me_3N\cdots BF_3$	0.74	0.96	2.57	2.05	2.81	5.24	6.11
$H_3N\cdots BH_3$	1.92	1.87	2.71	0.79	1.75	4.52	5.57
$Me_3N\cdots BH_3$	0.74	0.95	2.39	0.84	1.83	4.30	5.21
$H_3N\cdots BMe_3$	1.92	1.88	2.63	0.34	1.22	3.92	4.80
$Me_3N\cdots BMe_3$	0.74	1.04	2.28	0.39	1.28	3.65	4.60

[a] Gas-phase dipole moments are zero for all three acids.

TABLE 6: Computed Induced Dipole Moments (Debye) from Geometry Distortion, Charge Polarization, and Charge Transfer

complex	$\Delta\mu_{dist}$(B)[a]	$\Delta\mu_{pol}$(B)[a]	$\Delta\mu_{dist}$(A)[a]	$\Delta\mu_{pol}$(A)[a]	$\Delta\mu_{ct}$(AB)[a]
$N_2\cdots SO_3$	0.0	0.28	0.0	0.11	0.05
$HCN\cdots SO_3$	0.0	0.58	0.22	0.33	0.22
$MeCN\cdots SO_3$	0.0	0.80	0.30	0.41	0.32
$H_3N\cdots SO_3$	−0.13	0.89	1.09	1.05	2.08
$Me_3N\cdots SO_3$	−0.20	0.89	1.35	1.32	2.37
$HCN\cdots BF_3$	0.0	0.40	0.31	0.19	0.11
$MeCN\cdots BF_3$	0.0	0.57	0.42	0.24	0.15
$H_3N\cdots BF_3$	−0.07	0.90	1.85	0.67	1.00
$Me_3N\cdots BF_3$	0.22	1.61	2.05	0.76	0.87
$H_3N\cdots BH_3$	0.05	0.84	0.79	0.96	1.05
$Me_3N\cdots BH_3$	0.21	1.44	0.84	0.99	0.91
$H_3N\cdots BMe_3$	−0.04	0.75	0.34	0.88	0.88
$Me_3N\cdots BMe_3$	0.30	1.24	0.39	0.89	0.95

[a] A = Lewis acid, B = Lewis base, and AB = complex of A and B.

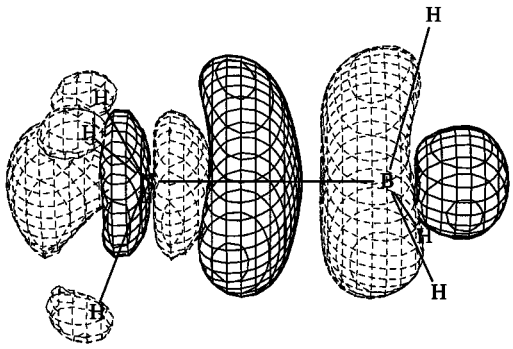

Figure 1. Electron density difference (EDD) maps in BH_3NH_3 due to polarization in going from the monomer species to the complex. The contour level is made at 0.005 e/au^3.

to illustrate the redistribution of the electron density due to these two effects separately. The electron density difference (EDD) between the initial block-localized wave function (eq 8) and the final block-localized wave function (eq 10) depicts the variation of electron density due to polarization by the other monomer in the complex. Figure 1 shows the polarization EDD map in BH_3NH_3. Clearly, the electron density of the NH_3 molecule is attracted toward BH_3. In contrast, the electron density of the monomer BH_3 moves away from the NH_3 monomer due to the repulsion from the nitrogen lone pair electrons. It is interesting to note that the result of this intramolecular charge polarization pattern is perfectly suited for charge-transfer

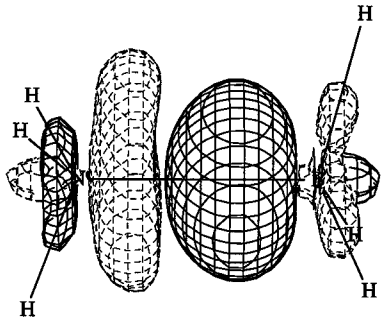

Figure 2. Electron density difference (EDD) maps in BH_3NH_3 due to charge transfer from NH_3 to BH_3 upon complex formation. The contour level is made at 0.005 e/au^3.

interactions and is presented in Figure 2. The EDD due to charge transfer from NH_3 to the empty p orbital of BH_3 is obtained by taking the difference of the electron density of the fully delocalized, adiabatic HF wave function and that of the BLW wave function (eq 11). The charge transfer occurs along the N−B bond in the direction from nitrogen to boron.

To quantify the amount of charge transferred, population analyses are employed, although it should be kept in mind that any population analysis schemes have advantages and disadvantages. Mulliken population analysis, which equally divides the overlap population to the bonding partners, is known for its sensitivity to the basis set used. On the other hand, natural population analysis (NPA) is less basis-set dependent.[34] Table 7 lists the computed total charges that the donor molecule possesses before (BLW wave function) and after (HF wave function) charge transfer is allowed in the calculation. The difference Δq represents the amount of charge density that is transferred from the donor to the acceptor.

By definition, in the block-localized wave function all block-localized MO's are expanded in the subspace of only one monomer and the electrons are therefore localized within each monomer, and the overlap population is zero. In the framework of Mulliken population analysis, the charge distribution in the HF wave function can be directly used to estimate the charge-transfer effect (i.e., $\Delta q = q_D$(HF)). On the other hand, the NPA is based on the overall electron density rather than individual orbitals, and the analysis on the BLW wave function of the donor molecule will lead to "residual" charges in the space of the acceptor monomer. This residual effect should be deducted from the total charge obtained using the delocalized HF wave function. In other words, the amount of charge transferred from

TABLE 7: Estimation of the Charge-Transfer Effect Using the HF/6-31G(d) Basis Function (All Charges in Electrons)

	natural population analysis		
D···A	q_D(BLW)[a]	q_D(HF)[a]	Δq
N_2···SO_3	0.001	0.003	0.002
HCN···SO_3	0.004	0.014	0.010
MeCN···SO_3	0.005	0.020	0.015
H_3N···SO_3	0.050	0.264	0.214
Me_3N···SO_3	0.058	0.322	0.264
HCN···BF_3	0.010	0.018	0.008
MeCN···BF_3	0.014	0.025	0.011
H_3N···BF_3	0.135	0.259	0.123
Me_3N···BF_3	0.123	0.245	0.122
H_3N···BH_3	0.193	0.319	0.126
Me_3N···BH_3	0.172	0.304	0.132
H_3N···BMe_3	0.190	0.29	0.109
Me_3N···BMe_3	0.147	0.265	0.117

[a] Charge for the donor. For the acceptor, $q_A = -q_D$.

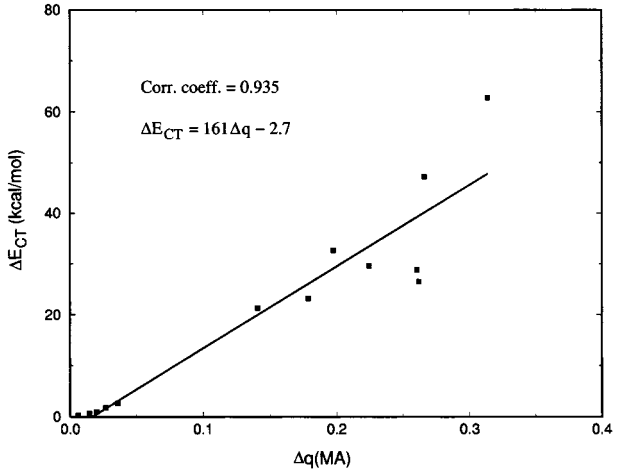

Figure 3. Correlation between the charge-transfer energy (ΔE_{CT}) and the amount of charge transfer Δq(MA) estimated with the Mulliken population analysis. Energies are given in kilocalories per mole and partial charges are given in electrons.

a Lewis base (donor) to a Lewis acid (acceptor) should be the population difference, i.e., $\Delta q = q_D(\text{HF}) - q_D(\text{BLW})$.

The data in Table 7 provide strong correlation between the amount of charge transfer and the strength of the basicity of the donor molecule and the acidity of the acceptor species. Clearly, nitrogen (N_2), hydrogen cyanide, and cyanomethane are much less basic than ammonia and its methyl derivatives since there is minimal charge transfer in these complexes, whereas the acidity decreases in the order $SO_3 > BH_3 > BF_3 > BMe_3$. In this rough correlation, it should also be remembered that steric effects play an additional role because bulky monomers tend to form complexes with longer donor−acceptor separations, leading to weaker overlap of orbitals and smaller charge transfer.

Timoshkin et al. and others showed that the experimentally derived linear correlation between charge transfer Δq and binding energy is not valid in cases examined in their study.[18] The present energy decomposition analyses reveal that polarization effects make significant contributions to redistribution of the electron density as well as the total binding energy. Thus, there is no theoretical guarantee that a linear relationship exists between the binding energy and the amount of charge transfer in the complex. However, the charge-transfer component of the binding energy may be related to the degree of the charge transfer. Figures 3 and 4 show the relationship between the charge-transfer energy and the amount of charge transferred

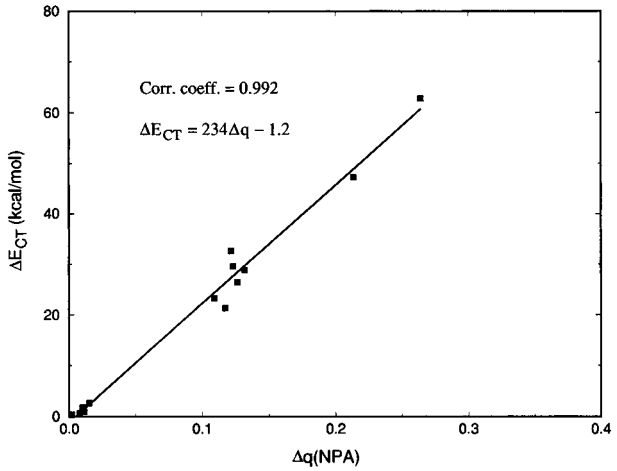

Figure 4. Correlation between the charge-transfer energy (ΔE_{CT}) and the degree of charge transfer Δq(NPA) estimated with the natural population analysis. Energies are given in kilocalories per mole and partial charges are given in electrons.

estimated by the Mulliken and NPA population schemes, respectively. Among the 13 complexes studied in this work, which cover an energy range −0.5 to −30 kcal/mol, we indeed find a linear correlation between ΔE_{CT} and Δq with excellent correlation coefficient (0.99 for the NPA results).

Conclusions

We have carried out an interaction energy decomposition analysis of a series of Lewis acid−base complexes, ranging from the weakly, nonbonded van der Waals complex regime to the strongly bonded complexes. The bonding character of these donor−acceptor complexes may be grouped into two categories: (I) weakly bonded complexes, which have characteristic interaction energies of 3−9 kcal/mol and monomer separations of 2.5−3.1 Å, and (II) strongly interacting complexes, which have binding energies more than 20 kcal/mol and shorter distances between the donor and acceptor molecules. The binding character of group I is primarily due to electrostatic interactions, while charge polarization and charge transfer between the two interacting monomers dominate the total binding interaction. It was also found that there is a good linear relationship between the amount of charge transfer from the donor molecule to the acceptor species in the complex with the charge-transfer energy; however, such a correlation is not guaranteed with the total binding energy because of the large contribution from the intramolecular polarization effect.

Acknowledgment. We thank the National Science Foundation and the University of Minnesota for support of this research. Discussions with Professor K. Leopold have been very helpful.

References and Notes

(1) Pauling, L. C. *The Nature of the Chemical Bond*, 3rd ed.; Cornell University Press: Ithaca, NY, 1960.

(2) Leopold, K. R.; Canagaratna, M.; Phillips, J. A. *Acc. Chem. Res.* **1997**, *30*, 57.

(3) Karpfen, A. *J. Phys. Chem. A* **2000**, *104*, 6871.

(4) Legon, A. C. *Angew. Chem., Int. Ed. Engl.* **1999**, *38*, 2687.

(5) Cassoux, P.; Kuczkowski, R. L.; Serafini, A. *Inorg. Chem.* **1977**, *16*, 3005.

(6) Muetterties, E. L. *The Chemistry of Boron and Its Compounds*; Wiley: New York, 1967.

(7) Janda, K. C.; Bernstein, L. S.; Steed, J. M.; Novick, S. E.; Klemperer, W. *J. Am. Chem. Soc.* **1978**, *100*, 8074.

(8) Kanda, F. A.; King, A. J. *J. Am. Chem. Soc.* **1951**, *73*, 2315.

(9) Bats, J. W.; Coppens, P.; Koetzle, T. F. *Acta Crystallogr.* **1977**, *B33*, 37.

(10) Canagaratna, M.; Phillips, J. A.; Goodfriend, H.; Leopold, K. R. *J. Am. Chem. Soc.* **1996**, *118*, 5290.

(11) Douglas, J. E.; Kenyon, G. L.; Kollman, P. A. *Chem. Phys. Lett.* **1978**, *57*, 553.

(12) Wong, M. W.; Wiberg, K. B.; Frisch, M. J. *J. Am. Chem. Soc.* **1992**, *114*, 523.

(13) For examples: (a) Anane, H.; Boutalib, A.; Nebot-Gil, I.; Tomas, F. *J. Phys. Chem. A* **1998**, *102*, 7073. (b) Karpfen, A. *Chem. Phys. Lett.* **2000**, *316*, 483. (c) Domene, C.; Fowler, P. W.; Legon, A. C. *Chem. Phys. Lett.* **1999**, *309*, 463. (d) Mennucci, B.; Cammi, R.; Tomasi, J. *Int. J. Quantum Chem.* **1999**, *75*, 767. (e) Rasul, G.; Prakash, G. K. S.; Olah, G. A. *J. Am. Chem. Soc.* **1999**, *121*, 7401. (f) Tarakeshwar, P.; Kim, K. S. *J. Phys. Chem. A* **1999**, *103*, 9116. (g) Vyboishchikov, S. F.; Frenking, G. *Theor. Chem. Acc.* **1999**, *102*, 300. (h) Fau, S.; Frenking, G. *Mol. Phys.* **1999**, *96*, 519. (i) Miller, N. E.; Wander, M. C.; Cave, R. J. *J. Phys. Chem. A* **1999**, *103*, 1084. (j) Davy, R. D.; Schaefer, H. F. *J. Phys. Chem. A* **1997**, *101*, 3135. (k) Frenking, G.; Dapprich, S.; Kohler, K. F.; Koch, W.; Collins, J. R. *Mol. Phys.* **1996**, *89*, 1245. (l) Hankinson, D. J.; Almlöf, J.; Leopold, K. R. *J. Phys. Chem.* **1996**, *100*, 6904. (m) Glendening, E. D.; Streitwieser, A. *J. Chem. Phys.* **1994**, *100*, 2900.

(14) (a) Pearson, R. G. *J. Am. Chem. Soc.* **1963**, *85*, 3533. (b) Pearson, R. G. *Chemical Hardness*; Wiley-VCH: Weinheim, 1997.

(15) Mulliken, R. S.; Person, W. B. *Molecular Complexes*; Wiley: New York:, 1969.

(16) Gurjanova, E. N.; Goldstein, I. P.; Romm, I. P. *Donor −Acceptor Bond*; Wiley: New York:, 1975.

(17) Jonas, V.; Frenking, G.; Reetz, M. T. *J. Am. Chem. Soc.* **1994**, *116*, 8741.

(18) Timoshkin, A. Y.; Suvorov, A. V.; Bettinger, H. F.; Schaefer, H. F. *J. Am. Chem. Soc.* **1999**, *121*, 5687.

(19) Thompson, W. H.; Hynes, J. T. *J. Am. Chem. Soc.* **2000**, *122*, 6278.

(20) Mo, Y.; Gao, J.; Peyerimhoff, S. D. *J. Chem. Phys.* **2000**, *112*, 5530.

(21) Mo, Y.; Subramanian, G.; Ferguson, D. M.; Gao, J. Submitted for publication.

(22) Fiacco, D. L.; Mo, Y.; Hunt, S. W.; Ott, M. E.; Roberts, A.; Leopold, K. R. *J. Phys. Chem. A* **2001**, *105*, 484.

(23) Leopold, K. R. In *Advances in Molecular Structure Research*; Hargittai, M., Hargittai, I., Eds.; JAI Press: Greenwich, CT, 1996; Vol. 2, p 103.

(24) Canagaratna, M.; Ott, M. E.; Leopold, K. R. *Chem. Phys. Lett.* **1997**, *281*.

(25) Burns, W. A.; Phillips, J. A.; Canagaratna, M.; Goodfriend, H.; Leopold, K. R. *J. Phys. Chem. A* **1999**, *103*, 7445.

(26) Fiacco, D. L.; Toro, A.; Leopold, K. R. *Inorg. Chem.* **2000**, *39*, 37.

(27) Boys, S. F.; Bernardi, F. *Mol. Phys.* **1970**, *19*, 553.

(28) Kestner, N. R.; Combariza, J. E. In *Reviews in Computational Chemistry*; Lipkowitz, K. B., Boyd, D. B., Eds.; Wiley: New York, 1999; Vol. 13, p 99.

(29) Mo, Y.; Peyerimhoff, S. D. *J. Chem. Phys.* **1998**, *109*, 1687.

(30) Mo, Y.; Zhang, Y.; Gao, J. *J. Am. Chem. Soc.* **1999**, *121*, 5737.

(31) Umeyama, H.; Morokuma, K. *J. Am. Chem. Soc.* **1977**, *99*, 1316.

(32) Mo, Y.; Gao, J. *BLW-ED*, 0.1 ed.; University of Minnesota: Minneapolis, MN, 2000.

(33) Frisch, M. J.; Trucks, G. W.; Schlegel, H. B.; Scuseria, G. E.; Robb, M. A.; Cheeseman, J. R.; Zakrzewski, V. G.; Montgomery, J. A. J.; Stratmann, R. E.; Burant, J. C.; Dapprich, S.; Millam, J. M.; Daniels, A. D.; Kudin, K. N.; Strain, M. C.; Farkas, O.; Tomasi, J.; Barone, V.; Cossi, M.; Cammi, R.; Mennucci, B.; Pomelli, C.; Adamo, C.; Clifford, S.; Ochterski, J.; Petersson, G. A.; Ayala, P. Y.; Cui, Q.; Morokuma, K.; Malick, D. K.; Rabuck, A. D.; Raghavachari, K.; Foresman, J. B.; Cioslowski, J.; Ortiz, J. V.; Baboul, A. G.; Stefanov, B. B.; Liu, G.; Liashenko, A.; Piskorz, P.; Komaromi, I.; Gomperts, R.; Martin, R. L.; Fox, D. J.; Keith, T.; Al-Laham, M. A.; Peng, C. Y.; Nanayakkara, A.; Challacombe, M.; Gill, P. M. W.; Johnson, B.; Chen, W.; Wong, M. W.; Andres, J. L.; Gonzalez, C.; Head-Gordon, M.; Replogle, E. S.; Pople, J. A. *Gaussian 98*, A.9 ed.; Gaussian, Inc.: Pittsburgh, PA, 1998.

(34) (a) Foster, J. P.; Weinhold, F. *J. Am. Chem. Soc.* **1980**, *102*, 7211. (b) Reed, A. E.; Weinhold, F. *J. Chem. Phys.* **1983**, *78*, 4066. (c) Reed, A. E.; Weinstock, R. B.; Weinhold, F. *J. Chem. Phys.* **1985**, *83*, 735. (d) Reed, A. E.; Weinhold, F.; Curtiss, L. A.; Pochatko, D. J. *J. Chem. Phys.* **1986**, *84*, 5687. (e) Reed, A. E.; Curtiss, L. A.; Weinhold, F. *Chem. Rev.* **1988**, *88*, 899.

(35) Townes, C. H.; Dailey, B. P. *J. Chem. Phys.* **1949**, *17*, 782.

(36) Lucken, E. A. C. *Nuclear Quadrupole Coupling Constants*; Academic Press: London, 1969.

(37) Gordy, W.; Cook, R. L. *Microwave Molecular Spectra*; Wiley: New York, 1984.